Reports of Biochemistry & Molecular Biology
Vol.12, No.1, Apr 2023

Original article

www.RBMB.net

Role of Cannabinoid Type 2 Receptor Activation in Renal Fibrosis Induced by Unilateral Ureteric Obstruction in Rats

Mahmoud El Tohamy*[1], Mohamed Adel[1], Fayza Rashad El-Menabawy[1], Gad El Mawla Gad[1], Randa El-Gamal[2], Hanaa El Serougy[1]

Abstract

Background: Chronic kidney disease (CKD) ends mostly with renal fibrosis. The effect of CB2 receptor on renal fibrosis has been unclear. The aim of this study was to investigate the effect of CB2 receptor on renal fibrosis and the mechanisms behind it.

Methods: 50 adult male Sprague-Dawley rats were divided into 5 groups; normal, sham; rats had their ureters only manipulated, UUO; rats had their left ureters ligated, and JWH post; rats had their left ureters ligated and they received JWH 133 for 14 days, JWH pre+post; rats received JWH 133 for 14 days before and after UUO procedure. Serum creatinine and BUN were assessed together with tissue MDA, GSH, and catalase. Histopathological evaluation of the renal tissue by H&E and Masson's trichrome was done. Immunohistochemical staining for TGF-β1, AQP1, Caspase-3, LC3B and p62 was performed. AQP1 and CB2 receptors genes expression was detected by quantitative RT-PCR.

Results: UUO had caused severe damage in the renal tissue with reduction of the renal function parameter accompanied by increase in the collagen deposition with increase TGF-β1 and decrease AQP1 expression.

Conclusions: The improvement of these parameters with JWH-133 suggests an anti-fibrotic role of CB2 receptor activation through reduction of oxidative stress, apoptosis, and autophagy.

Keywords: AQP1, CB2 receptor, JWH-133, Renal fibrosis, UUO.

Introduction

Chronic kidney disease (CKD) is characterized by gradual loss of renal function over time. It represents a serious hazard to human health due to its high prevalence and estimated to affect hundreds of millions of people (1). Fibrosis is the common end point event of various CKDs, and the extent of the fibrosis indicates the residual renal function. Fibrosis represents a series of dynamic processes including imbalance between the production and degradation of extracellular matrix, epithelial to mesenchymal transition (EMT) with loss of epithelial membrane protein such as AQP1, immune cell infiltration and fibroblast activation. The process of fibrosis is usually associated with oxidative stress, mitochondrial dysfunction and excessive apoptosis and autophagy. Intervention in the progression of renal fibrosis highlights a promising therapeutic target for CKDs (2).

A wide variety of experimental models are used to study the biochemical mechanisms leading to the progression of CKD to renal fibrosis. Urinary pathway obstruction, which may result either from the obstruction of one

1: Department of Medical Physiology, Faculty of Medicine, Mansoura University, Egypt.
2: Department of Biochemistry, Faculty of Medicine, Mansoura University, Egypt.
***Corresponding author: Mahmoud El Tohamy; Tel: +20 01005006843; E-mail: dr.m.eltohamy@mans.edu.eg.**
Received: 17 Nov, 2022; Accepted: 1 Feb, 2023

[DOI: 10.61186/rbmb.12.1.59]

or both ureters, provokes the progressive damage of renal structures, which leads to chronic renal dysfunction. In rodents, unilateral ureteric obstruction (UUO) can be considered the most widely used model to study the mechanisms behind the development of renal fibrosis (3).

On the other hand, the endocannabinoid system has been recognized as an endogenous lipid signaling system which is essential for immune function, energy expenditure and the regulation of food intake. The endocannabinoid system is comprised of endogenous lipid ligands, anandamide and 2-arachidonoyl glycerol, their cannabinoid 1 and cannabinoid 2 receptors (CB1 and CB2), and the enzymes involved in their biosynthesis and degradation. It is present in both the central nervous system and peripheral organs (4).

Cannabinoid 1 and cannabinoid 2 receptors (CB1 and CB2) are G protein-coupled receptors, which primarily couple to G proteins of the Gi and Go classes. These receptors activation exerts diverse consequences on cellular physiology, including synaptic transmission, gene transcription, cellular motility, etc. Although CB1 and CB2 receptors share some characteristics and signaling mechanisms, they are different in in tissue distribution. Whereas CB1 receptor is the most abundant in the CNS, the CB2 receptor is mainly expressed in the immune system but it may also be expressed in the nervous tissue, especially under certain pathological conditions (5). Many of the CB1 ligands have limited applications as a result of their psychoactive side effects, and therefore cannabinoid research has shifted to selective CB2 ligands (6).

Both CB1 and CB2 receptors are located in the normal kidney. Moreover, renal tissue is enriched with endocannabinoids, implying physiological relevance. CB2 receptors show a wide-spread expression pattern in different renal cells including glomerular podocytes and tubular epithelial cells (7). There is a growing belief about the potential involvement of CB1 and CB2 receptor in the pathogenesis of various renal disorders. While CB1 is consistently upregulated in a wide variety of kidney injury models such as diabetic nephropathy and UUO (8). Data on the expression of the CB2 receptor in CKD are contradictory. Some studies showed a possible protective effect of CB2 receptor activation on kidney structure and function in different animal model of kidney disorders (9, 10). Also, the anti-fibrotic effect of CB2 receptor agonists has been reported in many studies (11, 12). However, Zhou et al. had reported that Targeted inhibition of CB2 receptors could reduce renal fibrosis (7). Modulation of CB2 receptor is an interesting approach for neuroprotection, inflammation, pain, addictions, arthritis, and cancer, among other possible clinical applications with minimal side effects (13). So, in this study we tried to investigate the effect of cannabinoid type 2 receptor activation on unilateral ureteric obstruction (UUO) induced renal fibrosis in rats and the underlying mechanisms behind this effect.

Materials and Methods

Experimental Animals

This study was conducted on 50 adult male Sprague Dawley rats weighing 150-200 grams. Animals were bred and housed in the animal house of Medical Experimental Research Center (MERC), Mansoura faculty of medicine, Mansoura University. The experimental protocol was approved by (Mansoura faculty of medicine committee of animal care and ethics) on 31-10-2019 and given code number MDP/19.10.30.

Experimental design

Rats were divided into 5 groups as following:

1: Normal; in this group rats were housed normally,

2: Sham; in this group the rats had their left ureters manipulated but not ligated and they received a vehicle; Dimethyl sulfoxide (DMSO) by IP injection for 14 days,

[DOI: 10.61186/rbmb.12.1.59]

3: UUO; in this group the rats had their left ureters ligated at 2 points and they received a vehicle (DMSO) by IP injection for 14 days,
4: JWH post; in this group the rats had their left ureters ligated at 2 points and they received JWH 133; at a dose of 0.2 mg /kg/day dissolved in a vehicle (DMSO) according to the manufacturer's instruction by IP injection for 14 days (9),
5: JWH pre+post; in this group the rats received JWH 133; a potent CB2 receptor agonist at a dose of 0.2 mg /kg/day dissolved in a vehicle (DMSO) by IP injection for 14 days then their left ureters were ligated at 2 point and the injection had continued for another 14 days after the operation. JWH 133, a potent selective CB2 receptor agonist was obtained from Tocris Bioscience Co., England (Cat. No. 1343/10).

Unilateral Ureteric Obstruction (UUO) protocol
Unilateral Ureteric Obstruction (UUO) was performed one week after acclimatization. Briefly after induction of general anesthesia by intraperitoneal injection of a solution of ketamine/xylazine (80:8 mg/kg), the abdominal cavity was exposed via midline incision and the left ureter was ligated at 2 points with 4-0 silk. Sham-operated rats underwent the same procedure, except for the ligation of the left ureter. All rats had been given amikacin sulfate (6 mg/kg, intra-muscularly) before the operation (14). After the operation, the rats were placed in conditions of 12 hours light–dark cycles, temperature of 25 °C, humidity of 50%, adequate ventilation, noise-free, food and water ad libitum, and under continuous veterinary monitoring.

Animal euthanasia and collection of samples
On day 15 from the UUO operation rats were sacrificed after being fasted overnight using thiopental anesthesia by I.P injection at a dose of 30-40 mg/kg. Serum samples and tissue specimens were collected for further assessment. Cardiac puncture was performed to obtain blood samples from the heart. The left kidneys were carefully dissected out and longitudinally divided. Portion of the kidney was fixed in 10% formalin for histopathological examination. Another portion of the kidney was weighted and kept frozen at -20 °C for measuring tissue oxidative stress markers. Lastly, a portion of the kidney was preserved in RNA later.

Serum Creatinine and blood urea nitrogen (BUN)
After collection of the blood samples in test tubes, they were left to clot for 30 minutes at room temperature then centrifuged at 1968 G for 15 minutes in order to obtain serum samples which were frozen and stored at -20 ℃ till chemical analysis. Serum creatinine levels were measured for all groups by using Kits purchased from Bio-diagnostic, Egypt (CAT. No. CR 12 50). Serum BUN levels were measured for all groups by using Kits purchased from Bio-diagnostic, Egypt (CAT. No. UR 21 10).

Tissue oxidative stress markers: Malondialdehyde (MDA), Reduced glutathione (GSH) and Catalase
Portions of the kidneys were homogenized in 5 – 10 ml cold buffer (50 mM potassium phosphate, pH 7.5. 1mM EDTA) per gram tissue using tissue homogenizer. The homogenate was centrifuged at 1789 G for 15 min at 4 °C. Oxidative stress markers were detected in the resultant supernatant of kidney homogenate**.** The MDA level in the tissue homogenate was determined by using kits purchased from Bio-diagnostic, Egypt (CAT.No.MD 25 29). The GSH level was determined by using kits purchased from Bio-diagnostic, Egypt (CAT.No.GR 25 11). The catalase level was determined by using kits purchased from Bio-diagnostic, Egypt (CAT.No.CA 25 17).

Histopathological assessment
Samples obtained from the kidneys of the sacrificed rats were immediately scrubbed with normal saline and fixed using buffered neutral formalin (10%). After the tissue is fixed properly, the samples were prepared by making paraffin blocks and sectioned then stained with hematoxylin and eosin. Renal

[DOI: 10.61186/rbmb.12.1.59]

interstitial lesions were characterized by the degree of changes to the glomerulus and tubules. At least 10 randomly chosen non-overlapping fields of view at magnifications of x 100 and x 400 were observed and recorded for each section. Renal interstitial lesions were characterized by the degree of changes to the glomerulus and tubules and were graded on a scale from 0 to 4: 0, normal; 1, changes to < 25% of the field; 2, changes to 25–50% of the field; 3, changes to 50–75% of the field; and 4, changes to > 75% of the field (15).

Masson's trichrome staining

The degree of renal interstitial fibrosis was assessed by staining of the renal tissue with Masson's trichrome and evaluating the extent of collagen deposition observed at x 100 and x 400 magnifications. An image analysis using (image j software, imagej.nih.gov/ij/) was applied for the quantification of collagen deposition.

Immunohistochemical staining

We used The Poly-detector Plus 3, 3'-diaminobenzidine (DAB) Horseradish peroxidase (HRP) Brown Immunohistochemistry (IHC) detection system from Bio SB (Cat. No BSB- 0261), that allows for the demonstration of antigens in formalin-fixed paraffin-embedded according to manufacturer's instruction (16). For the evaluation of Caspase-3 we used rabbit monoclonal antibody, class IgG kit (Cell Signaling Technology® Cat. No. 9664). For the evaluation of transforming growth factor beta 1(TGF-β1) we used mouse monoclonal Antibody, class IgG kit (SANTA CRUZ BIOTECHNOLOGY, INC, Cat. No. sc-65378). We used rabbit polyclonal antibody, class IgG kits for the evaluation of aquaporin-1 (AQP1) (Cat. No. ab65837, Abcam, Cambridge, United Kingdom), LC3B (Cat. No. A5601, Abclonal, USA), and p62 (Cat. No. A7758, Abclonal, USA). IHC results were further assessed by morphometric analysis using Image J software. We measured the area percentage of Caspase-3, TGF-β1, AQP1, LC3B, and p62 immunoreactivity examined at high magnifications x400 (17).

Quantitative Real-Time PCR

RNA later was used to preserve samples of the renal tissue (10 ul per 1 mg of renal tissue) (catalog no. 76104, Qiagen, Germany). After submersion of the samples in RNA later, it was kept for 24 hours at 2-8 °C then stored at −80 °C and stored for further processing. Tissue samples were homogenized using five strokes of liquid nitrogen. RNA was extracted with the help of the QIAzol reagent (Cat. No. 79306, Qiagen, Germany). The resulting RNA was checked by Thermo-Scientific Nano Drop 2000 (USA) for confirmation of the purity and concentration. Formation of the first strand of cDNA from 1ug of RNA was achieved using Sensi FASTTM cDNA Synthesis Kit (Cat. No. 12594100) using Applied Biosystems 2720 Thermal-Cycler (Applied Biosystems, USA).

Amplification of cDNA templates was performed using a real-time PCR instrument (Pikoreal-96, Thermo-Scientific). The amplification reaction contained a 20 μl total volume mixture [10 μl of HERA-SYBR green PCR Master Mix (Willowfort, UK), 2 μl of cDNA template, 2 µl (10 pmol/ μl) gene primer and 6 μl of nuclease-free water]. The sequences of the used primer pairs are mentioned in (Table 1), Glyceraldehyde-3-phosphate dehydrogenase (GAPDH) was used as a reference gene. Primer specificity was confirmed using Primer-BLAST program (NCBI/primer-BLAST [https://www.ncbi.nlm.nih.gov/tools/primer-blast/]) Primers sets were synthesized by (Vivantis, Malaysia). The specificity of the PCR products was confirmed using melting curve analysis. Relative gene expression levels were represented as ΔCt = Ct target gene – Ct housekeeping gene; $2^{-\Delta\Delta CT}$ method was used to calculate the fold change of gene expression (18). PCR products were run on 3% agarose gels and visualized on UV transilluminator (OWI-Scientific, France). Then, the gels were photographed using BioRad gel documentation system (BioRad, USA).

[DOI: 10.61186/rbmb.12.1.59]

Table 1. The sequence of the primers used in qRT-PCR analysis.

Gene		Sequence	Product length (bp)	RefSeq	Reference
AQP1	**Forward**	GCT GTC ATG TAT ATC ATC GCC CAG	107	NM_012778.1	(19)
	Reverse	AGG TCA TTT CGG CCA AGT GAG T			
CB2	**Forward**	TGA CCG CTG TTG ACC GAT AC	200	NM_001164142.3	(20)
	Reverse	CAG GAG GTA GTC GTT GGG GAT			
GAPDH	**Forward**	TGC CAC TCA GAA GAC TGT GG	85	NM_017008.4	(21)

Statistical analysis

Statistical analysis of the results was performed by means of the statistical package for social science (spss) version 23. Normally distributed data was expressed as Mean ± SD, and Data were compared by Analysis of Variance (ANOVA) followed by post hoc Tukey test (level of significance at P value < 0.05) to compare between more than two groups of numerical (parametric) data. By means of Microsoft®Excel® for windows® (Microsoft Inc., USA), data were graphically represented.

Results

Serum creatinine and blood urea nitrogen (BUN) levels

Our results revealed a significant increase in the mean serum creatinine level when in UUO group compared to sham group (P< 0.001). However, this elevation was significantly reduced by IP injection of JWH 133 in JWH pre+post group (p = 0.003). Also, there was a significant elevation in serum BUN in UUO group when compared to sham group (P< 0.001). This elevation was also significant in JWH post and JWH pre+post groups when compared to sham group (P< 0.001) but still significantly lower than that of UUO group (p =0.018, p =0.002 respectively) (Table 2).

Tissue oxidative stress markers: MDA, GSH and catalase

Table 3 showed a significant increase in the mean tissue malondialdehyde level in UUO group (P< 0.001). This elevation was also significant in JWH post and JWH pre+post groups when compared to sham group (P< 0.001) but was significantly lower than that of UUO group (P< 0.001). On the other hand, GSH level and catalase activity appeared to be markedly reduced in UUO group. However, this reduction was also significantly reversed by IP injection of JWH 133 in JWH post and JWH pre+post groups (P< 0.001).

Table 2. Values of serum creatinine and blood urea nitrogen (BUN) among normal, sham, UUO (unilateral ureteric obstruction), JWH post and JWH pre+post groups.

Groups		Normal	Sham	UUO	JWH post	JWH pre+post
Creatinine (mg/dl)	Mean ± SD	0.457 ± 0.083	0.483 ± 0.057	^{ab} 0.854 ± 0.085	^{ab} 0.77 ± 0.069	^{abc} 0.718 ± 0.096
BUN (mg/dl)		25.69 ± 2.4	24.7 ± 3.66	^{ab} 43.76 ± 5.97	^{abc} 37.53 ± 4.43	^{abc} 35.89 ± 4.3

Analysis was done by One Way ANOVA with post hoc Tukey's Test. P value < 0.05 is considered significant. a = significance with normal group. b = significance with sham group. c = significance with UUO group.

Table 3. Values of tissue oxidative stress markers; malondialdehyde (MDA), reduced glutathione (GSH) and catalase levels among normal, sham, UUO (unilateral ureteric obstruction), JWH post and JWH pre+post groups.

Groups		Normal	Sham	UUO	JWH post	JWH pre+post
MDA (nmol/g. tissue)	Mean ± SD	0.208 ± 0.0475	0.191 ± 0.0463	^{ab} 0.47 ± 0.0968	^{abc} 0.343 ± 0.0506	^{abc} 0.32 ± 0.0467
GSH (nmol/g. tissue)		463.3 ± 31.6	456.7 ± 31.4	^{ab} 259.6 ± 29.4	^{abc} 333.2 ± 33.8	^{abc} 331.8 ± 31.4
Catalase (U/g. tissue)		8.74 ± 0.47	8.42 ± 0.43	^{ab} 4.01 ± 0.33	^{abc} 5.05 ± 0.49	^{abc} 5.06 ± 0.46

Analysis was done by One Way ANOVA with post hoc Tukey's Test. P value < 0.05 is considered significant. a = significance with normal group. b = significance with sham group. c = significance with UUO group.

[DOI: 10.61186/rbmb.12.1.59]

Histopathological evaluation

There was no difference between normal and sham groups as both of them show normal renal cortices and medulla (Fig. 1). On the other hand, the UUO group shows severe structural damage in the form of tubular dilation arrows), tubular atrophy, epithelial degeneration and tubular proteinaceous casts, and interstitial infiltration of inflammatory cells (Fig. 1). However, this sever damage was markedly alleviated by IP injection of JWH 133 as evident by the reduced structural damage including tubular dilation, epithelial degeneration and tubular proteinaceous casts, and interstitial inflammation. This was further confirmed by the histopathological scoring of the renal tissue lesions.

Histopathology of the renal tissue by Masson's trichrome

Masson's trichrome staining was used to evaluate the degree of renal interstitial fibrosis based on the extent of collagen deposition. Renal sections from normal and sham groups show minimal collagen deposition in cortices and medulla. Alternatively, stained renal cortices and medulla from UUO group show marked bluish collagen deposition in intersitium (Fig. 2). Both JWH post and JWH pre+post groups show significant reduction in renal interstitial fibrosis and percentage area of collagen deposition when compared to UUO group ($P< 0.001$). It is important to note that there was a significant reduction in collagen deposition surface area in JWH pre+post group when compared to JWH post group ($P< 0.001$) (Fig. 2).

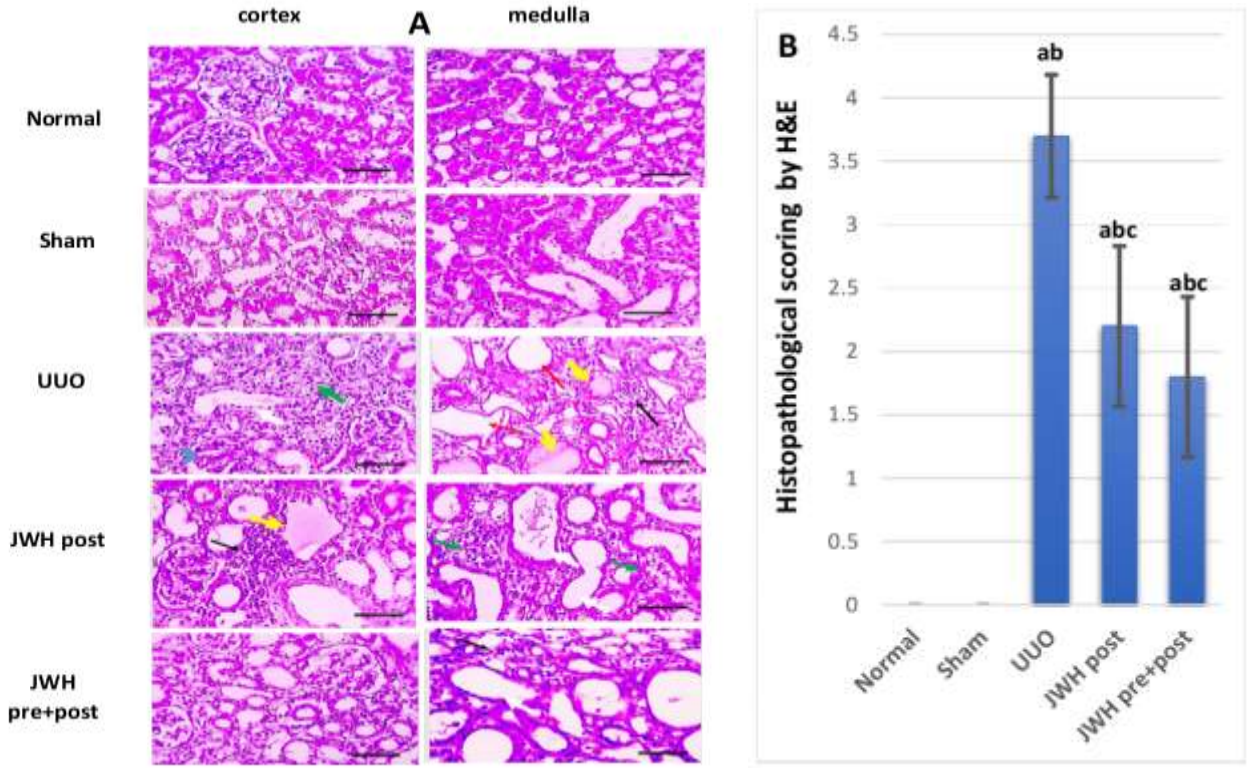

Fig. 1. A: Representative pictures of the H&E-stained renal cortices and medulla from normal, sham, UUO, JWH post and JWH pre+post groups examined at high magnifications (x400 Scale bar 50 µm) show structural damage such as tubular dilation (white arrows), tubular atrophy (red arrows), epithelial degeneration (green arrows) and tubular protenaceos casts (yellow arrows), interstitial infiltration of inflammatory cells (black arrows) and enlarged glomeruli (arrowheads). **B**: Histopathological scoring of the renal tissue damage by Hematoxylin & Eosin in normal, sham, UUO (unilateral ureteric obstruction), JWH post and JWH pre + post groups. Each group = 10 rats. P value < 0.05 is significant (One Way ANOVA with post hoc Tukey's Test). a = significance with Normal group. b = significance with Sham group. c = significance with UUO group.

[DOI: 10.61186/rbmb.12.1.59]

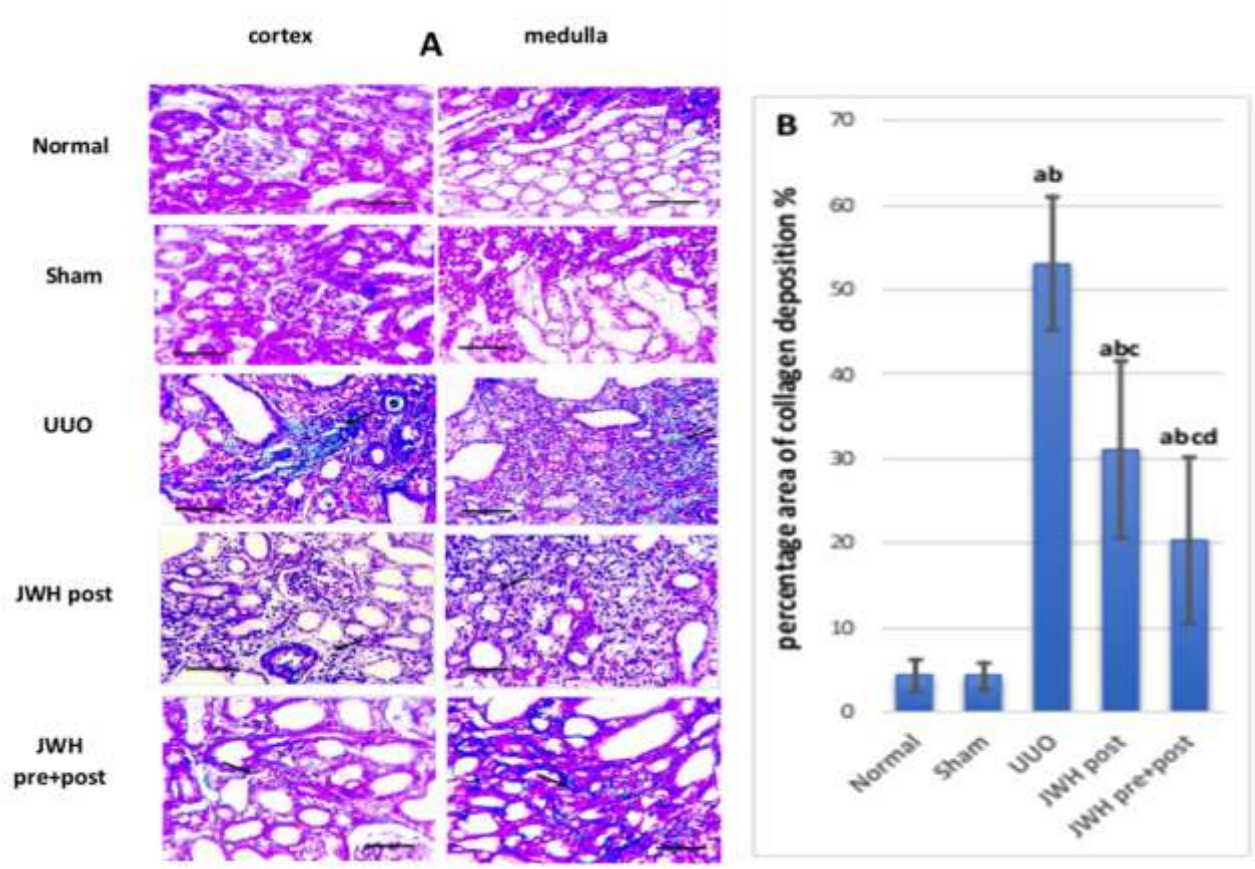

Fig. 2. A: Representative pictures of the Masson's trichrome stained renal sections from normal, sham, UUO, JWH post and JWH pre+post groups examined at high magnifications (x400 Scale bar 50 μm) showing marked bluish collagen deposition in intersitium of UUO group (black arrows). JWH post group showing reduced interstitial bluish collagen deposition (black arrows) when compared with untreated rats. Renal cortices and medulla from JWH pre+post group showing very little collagen deposition in intersitium (black arrows) when compared with untreated rats. B: percentage area of collagen deposition by Masson's Trichrome in Normal, Sham, UUO, JWH post and JWH pre + post groups. Each group = 10 rats. P value < 0.05 is significant (One Way ANOVA with post hoc Tukey's Test). a = significance with Normal group. b = significance with Sham group. c = significance with UUO group. d = significance with JWH post group.

Immunohistopathology for evaluation of TGF-β1, AQP1, Caspase-3, LC3B and p62

The expression of TGF-β1 was significantly higher in UUO group when compared to sham group (P< 0.001). However, it was significantly reduced in JWH post and JWH pre+post groups when compared to UUO group (P< 0.001) but still significantly higher than normal and sham group (P< 0.001) (Fig. 3). On the other hand, the expression of AQP1 was significantly reduced in UUO group when compared to sham group (P< 0.001). IP injection of JWH-133 has raised AQP1 expression in JWH post and JWH pre+post groups respectively when compared to UUO group (P< 0.001) but still significantly lower than normal and sham group (P< 0.001). Additionally, there was a significant increase in AQP1 expression in JWH pre+post group when compared to JWH post group (p =0.009) (Fig. 3).

The expression of caspase-3 was significantly higher in UUO group when compared to sham group (P< 0.001). JWH post and JWH pre+post groups show significantly lower expression when compared to UUO group (P< 0.001) but still significantly higher than Normal and Sham group (P< 0.001) (Fig. 4). As regard the autophagy markers LC3B and p62, the expression of LC3B was significantly higher in UUO group when compared to sham group (P< 0.001). Similarly, JWH-133 treated

[DOI: 10.61186/rbmb.12.1.59]

groups showed lower levels of LC3B expression than that of UUO group (Fig. 4). On the other hand, p62 was significantly reduced in UUO group when compared to sham group (P< 0.001). Also, JWH-133 had improved this reduction in JWH post and JWH pre+post groups but still significantly lower than normal and sham groups (P< 0.001) (Fig. 4).

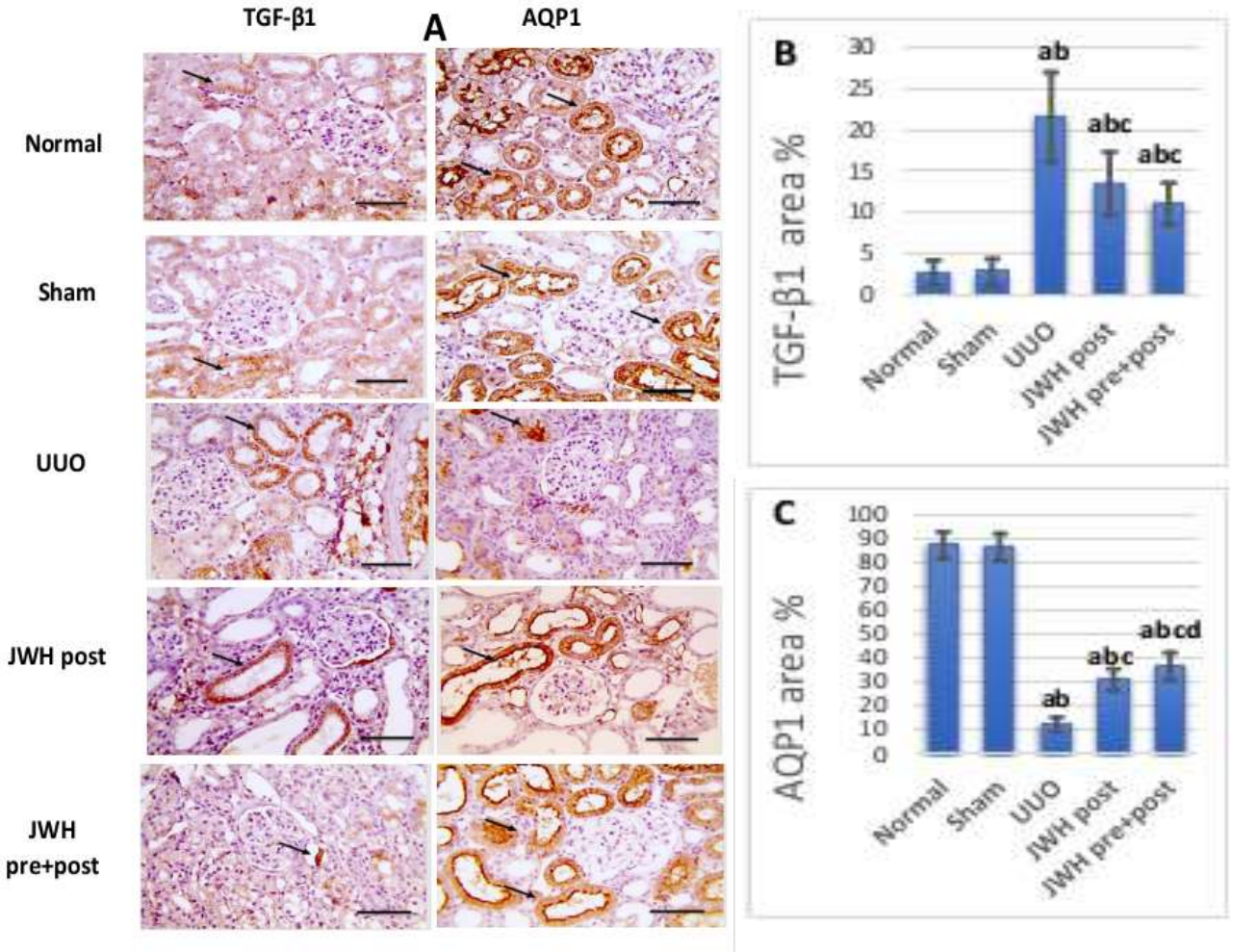

Fig. 3. A: Representative pictures of immunostained renal sections against TGF-β1 and AQP1 (examined at high magnifications x400 Scale bar 50 μm) from normal, sham, UUO, JWH post and JWH pre+post groups. examined at high magnifications (x400 Scale bar 50 μm). IHC counterstained with Mayer´s hematoxylin (arrows point to positive brown reaction), showing marked expression of TGF-β1 in UUO group when compared with other groups with reduced expression in JWH post and JWH pre+post groups. While AQP1stained sections show reduced expression in UUO group with partially restored expression in JWH post and JWH pre+post groups. **B-C**: Each group = 10 rats. P value < 0.05 is significant (One Way ANOVA with post hoc Tukey's Test). a = significance with normal group. b = significance with sham group. c = significance with UUO group. d = significance with JWH post group. **B**: Percentage area of TGF-β1 expression in normal, sham, UUO, JWH post and JWH pre + post groups. **C**: Percentage area of AQP1 expression in normal, sham, UUO, JWH post and JWH pre + post groups.

[DOI: 10.61186/rbmb.12.1.59]

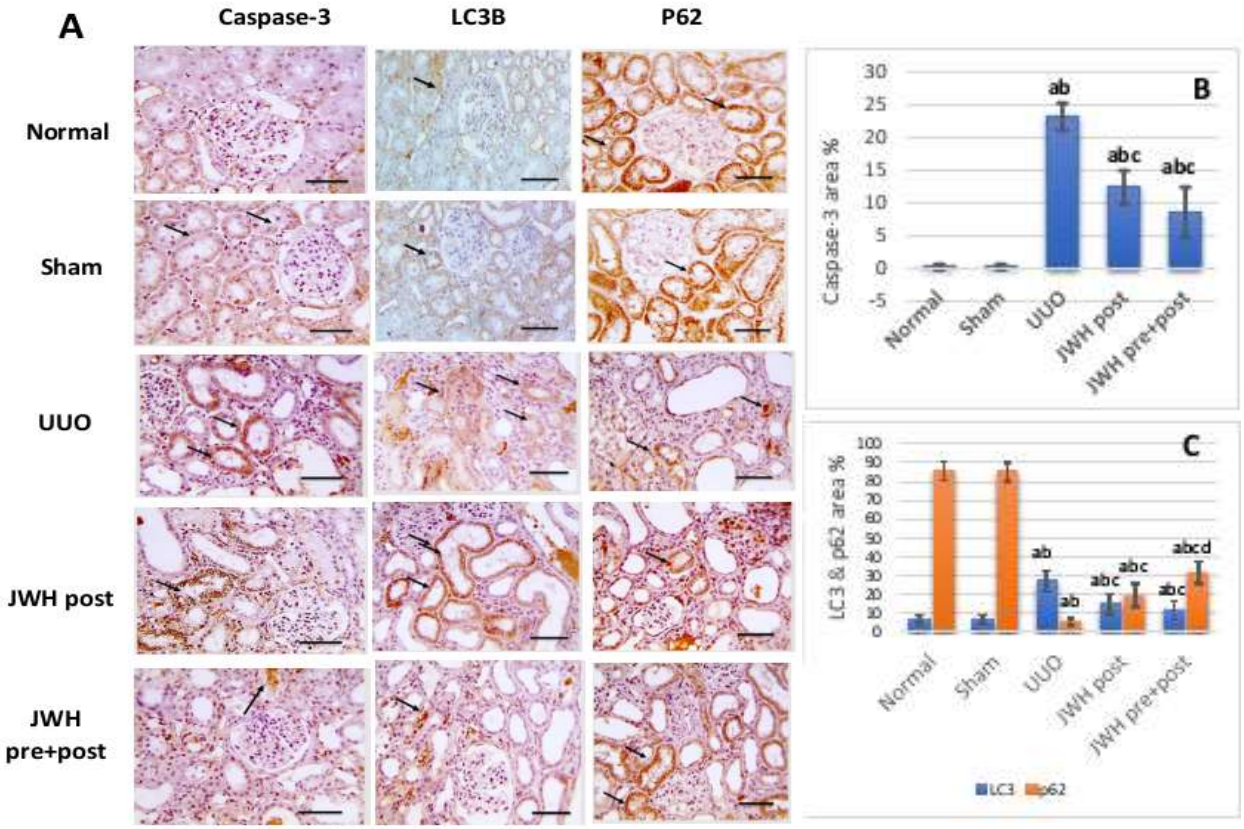

Fig. 4. A: Representative pictures of immunostained renal sections against Caspase-3, LC3B and p62 from normal, sham, UUO, JWH post and JWH pre+post groups. examined at high magnifications (x400 Scale bar 50 µm) IHC counterstained with Mayer´s hematoxylin (arrows point to positive brown reaction), showing marked expression of caspase-3 and LC3B in UUO group when compared with other groups with reduced expression in JWH post and JWH pre+post groups. group. While p62 stained sections show reduced expression in UUO group with partially restored expression in JWH post and JWH pre+post groups. **B-C**: Each group = 10 rats. P value < 0.05 is significant (One Way ANOVA with post hoc Tukey's Test). a = significance with normal group. b = significance with sham group. c = significance with UUO group. d = significance with JWH post group. **B**: Percentage area of Caspase-3 expression in normal, sham, UUO, JWH post and JWH pre + post groups. **C**: Percentage area of LC3B & p62 expression in normal, sham, UUO, JWH post and JWH pre + post groups.

Quantitative Real-Time PCR Evaluation of AQP1 and CB2 receptors genes expression

Our qPCR test had revealed a significant reduction in AQP1 gene expression in UUO group (P< 0.001). However, IP injection of JWH 133 had reverted this reduction and produced a marked elevation in AQP1 gene expression in both JWH post and JWH pre+post groups but still significantly lower than that of normal and sham groups (P< 0.001). There was no notable change between either normal and sham groups or JWH post and JWH pre+post groups (p =0.926, p =0. 759 respectively) (Fig. 5).

As regard CB2 receptor gene expression, there was no significant difference between UUO, JWH post and JWH pre+post groups. However, all these groups were markedly lower than normal and sham groups (Fig. 5).

[DOI: 10.61186/rbmb.12.1.59]

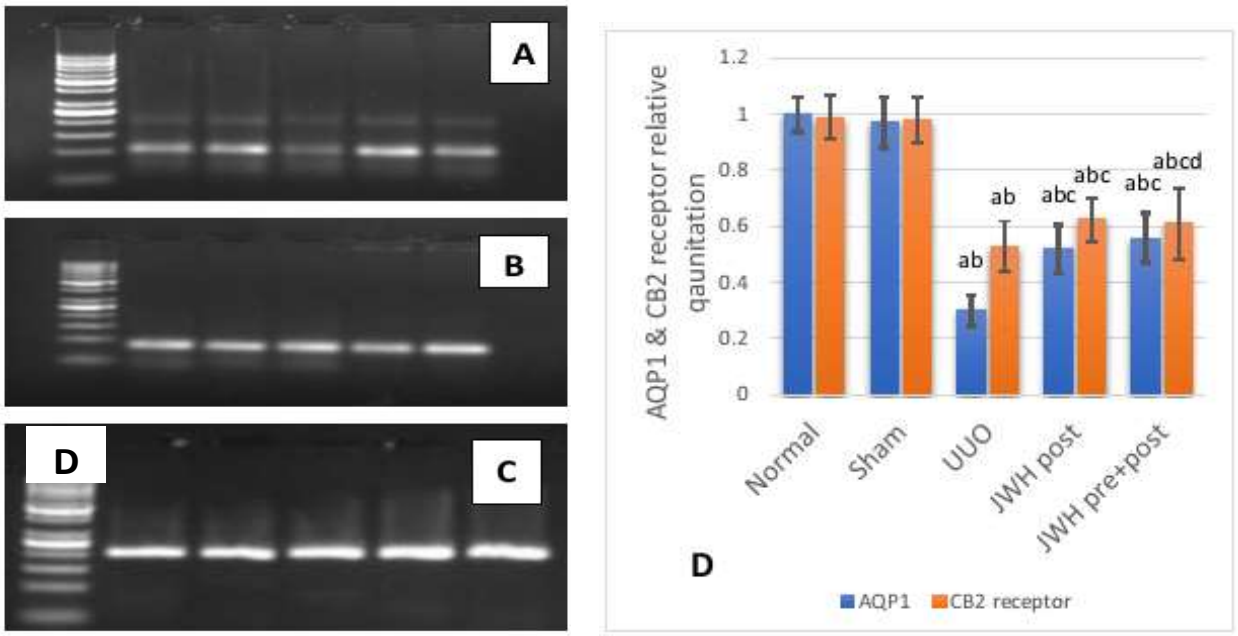

Fig. 5. A-C: Gel electrophoresis of the studied genes. Lane 1: 50bp ladder. Lane 2: normal group. Lane 3: sham group. Lane 4: UUO group. Lane 5: JWH post group. Lane 6: JWH pre+post group. **A**: AQP1 gene qPCR product (107 bp). **B**: CB2 receptor gene qPCR product (200bp). **C**: control gene (GAPDH) qPCR product (85bp). **D:** Relative quantitation (RQ) for AQP1 and CB2 receptor genes by real time qPCR in normal, sham, UUO (unilateral ureteric obstruction), JWH post, JWH pre+post groups. Each group = 10 rats. P value < 0.05 is significant (One Way ANOVA with post hoc Tukey's Test). a = significance with normal group. b = significance with sham group. c = significance with UUO group. d = significance with JWH post group.

Discussion

In order to achieve the aim of this study, a model of unilateral ureteric obstruction (UUO) was adopted. This model was preferred because of its accelerated time course and its ability to reproduce a fibrotic sequence of events that is very similar to what happens in humans (22). UUO group showed impaired renal function, as indicated by significant increases in serum creatinine and blood urea nitrogen (BUN) levels when compared to normal and sham groups (Table 2). These findings are in line with previous studies, and point towards the glomerular and tubular damage associated with ureteric obstruction (23). This reduced glomerular filtration of creatinine and BUN is possibly caused by reduced renal blood flow, renal vasoconstriction, tubular atrophy, and renal fibrosis subsequent to UUO (24).

The activation of CB2 by JWH-133 receptors has been shown to attenuate the changes in the renal function parameters when compared to UUO group (Table 2), implying that it could diminish renal injury and ameliorate renal dysfunction after UUO. Barutta et al. revealed that deletion of CB2 receptors during diabetic nephropathy worsened kidney function in a CB2 knockout mice model (25). Similar findings were postulated by several studies (26, 27). These results was also supported by histopathological examination of the renal tissue by Hematoxylin and Eosin with scoring of the lesions using the score system proposed by Shi et al. (15). Upon comparison, we have found that application of UUO has caused significant structural damage in both the cortex and medulla in the studied renal tissue samples (Fig. 1).

The use of JWH-133 as an agonist for CB2 receptor in JWH post and JWH pre+post has caused marked reduction in the microscopic structural damage with fewer dilated tubules,

[DOI: 10.61186/rbmb.12.1.59]

less substantially atrophied parenchyma and mild interstitial inflammation (Fig. 1). Çakır et al. has stated that CB2 receptor agonist JWH-133 had reduced the inflammatory cells infiltration and glomerular and tubular damage through the reduction of pro inflammatory cytokine tumor necrosis factor alpha (TNF-α), Interleukin 1 beta (IL-1β), and IL-6 (27). It is well documented that activation of CB2 receptor reduces inflammatory response in various inflammatory associated diseases including nephropathy and cystitis (28, 29).

In order to assess the degree of fibrosis, our study implemented the evaluation of collagen deposition together with transforming growth factor beta 1 (TGF-β1) and Aquaporin1 (AQP1) expression. The histopathological examination of the renal tissue by Masson's Trichrome revealed a significant increase in percentage area of fibrosis which was marked by increased collagen deposition in the UUO group. Indeed, activation of CB2 receptor by JWH-133 had significantly reduced the area of fibrosis following the obstruction. Our result also showed that it was more effective in reducing the fibrosis when used before and after the UUO procedure in JWH pre+post group (Fig. 2) indicating a possible preventive on top of a curative effect of CB2 receptor stimulation. These findings were further confirmed by the immunohistopathological evaluation of the pro-fibrotic factor TGF-β1. Similarly, there was a marked increase in TGF-β1 expression in UUO group and CB2 receptor activation had also reduced its expression (Fig. 2).

Fibroblasts are predominant cells during the process of fibrosis. They acquire a contractile phenotype and transform into myofibroblasts, which expresses α-SMA and responsible for depositing extracellular matrix formed of high concentrations of collagens. This activation is strongly induced by TGF-β (30). In vitro study in a primary culture of human fibroblasts showed that CB2 receptor activation with JWH-133 reduces α-SMA expression and collagen production in human fibroblasts under stimulation with TGF-β (31). Similarly, Lecru et al. had shown that treatment with the CB2 agonist reduced fibrosis while the antagonist aggravated it (32). Our results is also supported by the fact that the antifibrotic effect of CB2 receptor has been reported in different body organs (33, 34).

An in vitro study by Li et al. implied that AQP1 might be an indicator for EMT which in turn reflects the extent of renal fibrosis (35). Our study revealed a significant reduction in the expression of AQP1 by Immunohistopathological staining in UUO group. This reduction was attenuated upon activation of CB2 receptor in JWH post and JWH pre+post groups (Fig. 2). This was, furthermore, confirmed by quantitative real-time PCR evaluation of AQP1 gene expression which has given the same result (Fig. 5).

These findings further support our suggestion that CB2 receptor agonists could be considered as anti-fibrotic agents. Our results are in direct contradiction with Zhou et al. (7) who explained that the reported protective effect of CB2 receptor activation in the previously mentioned studies could be attributed to high sequence homology between CB1 and CB2, and the possible off-target effect, of any inhibitors and agonists to these receptors. Therefore, in this study we used JWH-133 ; a potent CB2 receptor agonist with a 35- to 40-fold selectivity for CB2 over CB1 receptors (36). Moreover, we avoided the use of a high dose of JWH-133 to prevent the cross activation of CB1 receptor which have been reported to have a pro-fibrotic effect (32).

Our results have shown that UUO leads to imbalance between the oxidant and antioxidant markers. The renal tissue level of catalase and GSH as enzymatic and non-enzymatic antioxidants respectively has been reduced in UUO group with concomitant elevation in the tissue MDA level. This imbalance was partially restored in rats receiving JWH-133 in JWH post and JWH pre+post groups (Table 3). CB2 receptor activation result in blocking mitogen-activated protein (MAP) kinase and the transcription factor; nuclear factor kappa B

[DOI: 10.61186/rbmb.12.1.59]

(NF-κB) activation, which leads to suppression of Nitric oxide synthase expression and NO production (37).

Caspase-3 is considered to be a major executioner protease which is essential for apoptotic death in mammalian cells (38). Interestingly, treatment with JWH-133 had caused significant reduction in caspase -3 expression percentage area (Fig. 3). Our results are in agreement with Çakır et al. (27) and Mukhopadhyay et al. (26) who claimed that CB2 receptor activation exerts its anti-apoptotic effect through reduction of caspase 3/7 activity and DNA fragmentation.

Indeed, the anti-apoptotic effect exerted by JWH-133 in this study is in line with its effect on expression of autophagy markers LC3B and p62 which were assessed to investigate the involvement of autophagy as a possible mechanism for the anti-fibrotic and protective effect of CB2 receptor activation in renal fibrosis. The autophagy pathway involves conjugation of microtubule-associated protein 1 light chain 3 (LC3-I) to the membrane lipid phosphatidyl- ethanolamine to form LC3-II (39). LC3-II is present on both the inner and outer isolation membranes, acting as a recognition site for LC3-binding chaperones such as p62/SQSTM1 (p62) which deliver their cargo to the autophagosome. p62 is removed from the cytoplasm mainly by autophagy, its amount is generally considered to inversely correlate with autophagic activity (40).

Our study had revealed a significant elevation in the autophagy executioner LC3B together with marked reduction in the autophagy consumed p62 upon ureteric obstruction. However, the activation of CB2 receptor has attenuated the increase in LC3B and the decrease in p62 in JWH post and JWH pre+post groups when compared to UUO group (Fig. 4)

Autophagy has been suggested to induce tubular atrophy and decomposition to promote renal fibrosis (41). Livingston et al. showed that a significant increase in LC3B was detected, while there was degradation of p62 after 2 weeks of UUO (42). On the other hand, autophagy has been reported to cause degradation of collagen I and active TGF-β1 thus inhibiting renal fibrosis (43). To the best of our knowledge, the link between CB2 receptor activation and autophagy and its role in renal fibrosis has not been discussed. However, a protective role of CB2 receptor was reported in different body organs through induction of autophagy rather than inhibiting it (44, 45). Such controversy may provide an interesting point for investigation throughout future research.

In conclusion, unilateral ureteric obstruction had caused severe damage in the renal tissue with reduction of the renal function parameter accompanied by increase in the collagen deposition with increase TGF-β1 and decrease AQP1 expression as markers of renal fibrosis. The improvement of these parameters with JWH-133; CB2 recebtor agonist suggests an anti-fibrotic role of CB2 receptor activation. Such role could be mediated through enhancing the anti-oxidative machinary of the cell; as evident by the increased level of GSH and catalase with reduction in the level of MDA. Another possible mechanism for this effect could be through reducing the expression of apoptotic excutioner protein caspase-3. Finally, the reduction in autophagy as evident by decreasing the expressin of LC3B and increasing the expression of p62 could provide a possible mechanism for this effect however, further investigation may be needed.

Acknowledgements

We acknowledged Dr Walaa Fekry Awadin for the pathological analysis, Dr Samah Fouad for the veterinary care and our Physiology Department for the significant support and assistance in the experimental part of the present study.

Funding

This research work was self-funded.

Conflicts of Interest

The authors declare that there is no conflict of interest.

[DOI: 10.61186/rbmb.12.1.59]

References

1. Shawky SA, Gaber O, Mostafa E, Sarhan WM. Uncoupling Protein 2 Expression Modulates Obesity in Chronic Kidney Disease Patients. Rep Biochem Mol Biol. 2021;10(1):119-25.
2. Zhao HY, Li HY, Jin J, Jin JZ, Zhang LY, Xuan MY, et al. L-carnitine treatment attenuates renal tubulointerstitial fibrosis induced by unilateral ureteral obstruction. Korean J Intern Med. 2021;36(Suppl 1):S180.
3. Grande MT, Pérez-Barriocanal F, López-Novoa JM. Role of inflammation in tubulo-interstitial damage associated to obstructive nephropathy. J Inflamm (Lond). 2010;7(1):19.
4. Tam J. The emerging role of the endocannabinoid system in the pathogenesis and treatment of kidney diseases. J Basic Clin Physiol Pharmacol. 2016;27(3):267-76.
5. Lu H-C, Mackie K. An introduction to the endogenous cannabinoid system. Biol Psychiatry. 2016;79(7):516-25.
6. Parastouei K, Aarabi MH, Hamidi GA, Nasehi Z, Kabiri-Arani S, Jozi F, et al. A CB2 Receptor Agonist Reduces the Production of Inflammatory Mediators and Improves Locomotor Activity in Experimental Autoimmune Encephalomyelitis. Rep Biochem Mol Biol. 2022;11(1):1-9.
7. Zhou L, Zhou S, Yang P, Tian Y, Feng Z, Xie X-Q, et al. Targeted inhibition of the type 2 cannabinoid receptor is a novel approach to reduce renal fibrosis. Kidney Int. 2018;94(4):756-72.
8. Barutta F, Corbelli A, Mastrocola R, Gambino R, Di Marzo V, Pinach S, et al. Cannabinoid receptor 1 blockade ameliorates albuminuria in experimental diabetic nephropathy. Diabetes. 2010;59(4):1046-54.
9. Çakır M, Tekin S, Doğanyiğit Z, Çakan P, Kaymak E. The protective effect of cannabinoid type 2 receptor activation on renal ischemia–reperfusion injury. Mol Cell Biochem. 2019:1-10.
10. Swanson ML, Regner KR, Moore BM, Park F. Cannabinoid Type 2 Receptor Activation Reduces the Progression of Kidney Fibrosis Using a Mouse Model of Unilateral Ureteral Obstruction. Cannabis Cannabinoid Res. 2022.
11. Tan Q, Chen Q, Feng Z, Shi X, Tang J, Tao Y, et al. Cannabinoid receptor 2 activation restricts fibrosis and alleviates hydrocephalus after intraventricular hemorrhage. Brain Res. 2017;1654:24-33.
12. Yang C-Y, Chau Y-P, Chen A, Lee OK-S, Tarng D-C, Yang A-H. Targeting cannabinoid signaling for peritoneal dialysis-induced oxidative stress and fibrosis. World J Nephrol. 2017;6(3):111.
13. Dhopeshwarkar A, Mackie K. CB2 Cannabinoid receptors as a therapeutic target—what does the future hold? Mol Pharmacol. 2014;86(4):430-7.
14. Figueroa SM, Lozano M, Lobos C, Hennrikus MT, Gonzalez AA, Amador CA. Upregulation of Cortical Renin and Downregulation of Medullary (Pro) Renin Receptor in Unilateral Ureteral Obstruction. Front Pharmacol. 2019;10:1314.
15. Shi Z, Wang Q, Zhang Y, Jiang D. Extracellular vesicles produced by bone marrow mesenchymal stem cells attenuate renal fibrosis, in part by inhibiting the RhoA/ROCK pathway, in a UUO rat model. Stem Cell Res Ther. 2020;11(1):1-21.
16. Panel BBR. Guidelines for safe work practices in human and animal medical diagnostic laboratories. MMWR Suppl. 2012;61:357-63.
17. Schneider CA, Rasband WS, Eliceiri KW. NIH Image to ImageJ: 25 years of image analysis. Nat Methods. 2012;9(7):671-5.
18. Freeman TC, Lee K, Richardson PJ. Analysis of gene expression in single cells. Current opinion in biotechnology. 1999;10(6):579-82.
19. Bouley R, Palomino Z, Tang S-S, Nunes P, Kobori H, Lu HA, et al. Angiotensin II and hypertonicity modulate proximal tubular aquaporin 1 expression. Am J Physiol Renal Physiol. 2009;297(6):F1575-F86.
20. Zhang M, Shi X, Wu J, Wang Y, Lin J, Zhao Y, et al. CoCl2 induced hypoxia enhances osteogenesis of rat bone marrow

[DOI: 10.61186/rbmb.12.1.59]

mesenchymal stem cells through cannabinoid receptor 2. Arch Oral Biol. 2019;108:104525.
21. Lai KN, Leung JC, Chan LY, Saleem MA, Mathieson PW, Tam KY, et al. Podocyte injury induced by mesangial-derived cytokines in IgA nephropathy. Nephrol Dial Transplant. 2009;24(1):62-72.
22. Nogueira A, Pires MJ, Oliveira PA. Pathophysiological mechanisms of renal fibrosis: a review of animal models and therapeutic strategies. in vivo. 2017;31(1):1-22.
23. Zhao D, Luan Z. Oleanolic acid attenuates renal fibrosis through TGF-β/Smad pathway in a rat model of unilateral ureteral obstruction. Evid Based Complement Alternat Med 2020;2020.
24. Chaabane W, Praddaude F, Buleon M, Jaafar A, Vallet M, Rischmann P, et al. Renal functional decline and glomerulotubular injury are arrested but not restored by release of unilateral ureteral obstruction (UUO). Am J Physiol Renal Physiol. 2013;304(4):F432-F9.
25. Barutta F, Grimaldi S, Franco I, Bellini S, Gambino R, Pinach S, et al. Deficiency of cannabinoid receptor of type 2 worsens renal functional and structural abnormalities in streptozotocin-induced diabetic mice. Kidney Int. 2014;86(5):979-90.
26. Mukhopadhyay P, Baggelaar M, Erdelyi K, Cao Z, Cinar R, Fezza F, et al. The novel, orally available and peripherally restricted selective cannabinoid CB2 receptor agonist LEI-101 prevents cisplatin-induced nephrotoxicity. Br J Pharmacol. 2016;173(3):446-58.
27. Çakır M, Tekin S, Doğanyiğit Z, Çakan P, Kaymak E. The protective effect of cannabinoid type 2 receptor activation on renal ischemia–reperfusion injury. Mol Cell Biochem. 2019;462.
28. Mukhopadhyay P, Pan H, Rajesh M, Bátkai S, Patel V, Harvey-White J, et al. CB1 cannabinoid receptors promote oxidative/nitrosative stress, inflammation and cell death in a murine nephropathy model. Br J Pharmacol. 2010;160(3):657-68.
29. Wang Z-Y, Wang P, Bjorling DE. Treatment with a cannabinoid receptor 2 agonist decreases severity of established cystitis. J Urol. 2014;191(4):1153-8.
30. Biernacka A, Dobaczewski M, Frangogiannis NG. TGF-β signaling in fibrosis. Growth Factors
. 2011;29(5):196-202.
31. Correia-Sá I, Carvalho C, A. Machado V, Carvalho S, Serrão P, Marques M, et al. Targeting cannabinoid receptor 2 (CB2) limits collagen production—An in vitro study in a primary culture of human fibroblasts. Fundam Clin Pharmacol. 2022;36(1):89-99.
32. Lecru L, Desterke C, Grassin-Delyle S, Chatziantoniou C, Vandermeersch S, Devocelle A, et al. Cannabinoid receptor 1 is a major mediator of renal fibrosis. Kidney Int. 2015;88(1):72-84.
33. Muñoz-Luque J, Ros J, Fernández-Varo G, Tugues S, Morales-Ruiz M, Alvarez CE, et al. Regression of fibrosis after chronic stimulation of cannabinoid CB2 receptor in cirrhotic rats. J Pharmacol Exp Ther. 2008;324(2):475-83.
34. Du W, Zhang T, Yang F, Gul A, Tang Z, Zhang H, et al. Endocannabinoid signalling/cannabinoid receptor 2 is involved in icariin-mediated protective effects against bleomycin-induced pulmonary fibrosis. Phytomedicine. 2022:154187.
35. Li J, Zhang M, Mao Y, Li Y, Zhang X, Peng X, et al. The potential role of aquaporin 1 on aristolochic acid I induced epithelial mesenchymal transition on HK-2 cells. J Cell Physiol. 2018;233(6):4919-25.
36. Tao Y, Tang J, Chen Q, Guo J, Li L, Yang L, et al. Cannabinoid CB2 receptor stimulation attenuates brain edema and neurological deficits in a germinal matrix hemorrhage rat model. Brain Res. 2015;1602:127-35.
37. Esposito G, De Filippis D, Maiuri MC, De Stefano D, Carnuccio R, Iuvone T. Cannabidiol inhibits inducible nitric oxide synthase protein expression and nitric oxide production in β-amyloid stimulated PC12 neurons through p38 MAP kinase and NF-κB involvement. Neurosci Lett. 2006;399(1-2):91-5.
38. Katunuma N, Matsui A, Le Q, Utsumi K, Salvesen G, Ohashi A. Novel procaspase- 3

[DOI: 10.61186/rbmb.12.1.59]

activating cascade mediated by lysoapoptases and its biological significances in apoptosis. Adv Enzyme Regul. 2001;41(1):237-50.
39. Ichimura Y, Kirisako T, Takao T, Satomi Y, Shimonishi Y, Ishihara N, et al. A ubiquitin-like system mediates protein lipidation. Nature. 2000;408(6811):488-92.
40. Pircs K, Nagy P, Varga A, Venkei Z, Erdi B, Hegedus K, et al. Advantages and limitations of different p62-based assays for estimating autophagic activity in Drosophila. PLoS One. 2012.
41. Forbes MS, Thornhill BA, Chevalier RL. Proximal tubular injury and rapid formation of atubular glomeruli in mice with unilateral ureteral obstruction: a new look at an old model. Am J Physiol Renal Physiol. 2011;301(1):F110-F7.
42. Livingston MJ, Ding H-F, Huang S, Hill JA, Yin X-M, Dong Z. Persistent activation of autophagy in kidney tubular cells promotes renal interstitial fibrosis during unilateral ureteral obstruction. Autophagy. 2016;12(6):976-98.
43. Ding Y, ll Kim S, Lee S-Y, Koo JK, Wang Z, Choi ME. Autophagy regulates TGF-β expression and suppresses kidney fibrosis induced by unilateral ureteral obstruction. J Am Soc Nephrol. 2014;25(12):2835-46.
44. Liu A, Yuan Q, Zhang B, Yang L, He Q, Chen K, et al. Cannabinoid receptor 2 activation alleviates septic lung injury by promoting autophagy via inhibition of inflammatory mediator release. Cell Signal. 2020;69:109556.
45. Liu W, Chen C, Gu X, Zhang L, Mao X, Chen Z, et al. AM1241 alleviates myocardial ischemia-reperfusion injury in rats by enhancing Pink1/Parkin-mediated autophagy. Life Sci. 2021;272:119228.

[DOI: 10.61186/rbmb.12.1.59]